

A Novel and Facile Method to Fabricate SiO₂ Nano-pillar Arrays on Glass Surface

H B Xu¹, J Zhang¹, Y Huang^{1,2}, Z H Zhou^{1,2,*} and S Shen³

¹College of Materials, Xiamen University, Xiamen, Fujian, China 361005

²Fujian Key Laboratory of Advanced Materials, Xiamen, Fujian, China 361005

³CSIRO Manufacturing, Clayton, VIC 3168, Australia

Corresponding author and e-mail: Z H Zhou, zzh@xmu.edu.cn

Abstract. SiO₂ regular nano-pillar arrays have been successfully fabricated on glass substrates by imprinting anodized nanoporous aluminum oxide (AAO) templates on inorganic SiO₂ sol coatings. The prepared SiO₂ nano-pillar array by using a template with the pore diameter of 43.01 nm shows an average pillar diameter of 48.78 nm, a surface roughness of 33.1 nm and a static water contact angle of 150.47°. Surface roughness of SiO₂ nano-pillar arrays can be adjusted by changing pore size of AAO templates and increases with the decrease of pore diameter of AAO templates. Transparent superhydrophobic glass is obtained when the prepared nano-pillar array is modified by fluoroalkylsilane, presenting a new way of preparing superhydrophobic glass.

1. Introduction

In recent years, transparent superhydrophobic surfaces have received extensive attention [1-4] due to their transparent, self-cleaning and anti-icing properties, and their potential applications on automotive, building and solar cell glass. Two requirements for superhydrophobic surface are surface roughness and low surface energy [5]. Rough surface structures are usually constructed with nanoparticles [6,7], nanopits [8], nanofibers [9], nanopillars [10,11], nanocones [12] and the like. Nanopillars and nanocones with the effect of anti-reflection and increasing visible light transmittance have great advantages in the preparation of transparent superhydrophobic glass.

There are two methods reported for preparing superhydrophobic nano-pillar arrays on glass substrates, one of which is patterned etching of glass surface to prepare glass nano-pillar arrays. Kim et al. [10] used nano-imprint lithography technology with anodized nanoporous alumina oxide (AAO) as template to form a Cr mask pattern on glass and then used inductively coupled plasma dry etching process to produce transparent superhydrophobic glass composed of nano-pillar array. Son et al. [13] produced an AAO mask pattern on glass by E-beam evaporation and anodizing technologies, and then prepared nano-pillar array using a dry etching process. However, patterned etching process on glass surface is complicated and requires expensive instruments, which limits its practical applications. Another method is to prepare nanopillars by embossing AAO templates on organic coatings on glass surface. Cho et al. [11] prepared superhydrophobic glass consisting of polydimethylsiloxane nano-pillar array with contact angle as high as 163.4° by using PDMS as coating material and AAO as template; Liu et al. [14] successfully prepared polyimide nano-pillar

structural superhydrophobic glass with PI coating and AAO template; Lee et al. [15] produced transparent superhydrophobic glass consisting of polystyrene nano-pillar array with PS as coating material by hot-pressing process with AAO template. This method is relatively simple, but organic nanopillars have various weaknesses, such as poor adhesion on glass substrate, and degradation during long-term use. As far as our knowledge, there are few reports about SiO₂ nano-pillar arrays prepared by AAO template imprinting method.

In this work, we report a novel and facile method to fabricate SiO₂ nano-pillar arrays on glass surface by using acidic SiO₂ sol as coating material and AAO as template. By changing pore size of AAO templates, a series of SiO₂ nanopillar structural rough surfaces with controllable morphologies can be obtained.

2. Experimental

Single-pass nanoporous alumina oxide templates (Shenzhen Topology Technology Co., Ltd.) were used as received. The template includes three-layer structure consisting of a regular AAO porous layer (effective AAO layer), an intermediate Al base and a back random AAO layer. Acidic SiO₂ sol, which preparation details had been described in our previous report [16], was obtained by acid hydrolysis of tetraethyl orthosilicate in a water-ethanol solution containing nitric acid and a coupling agent (KH560) was added as a binder.

The SiO₂ sol was spin-coated on a clean glass substrate (3.2 mm float green glass) at 380 rpm for 10 sec, and after aging in air for 6-8 min, an AAO template was placed on the coating and slowly pressed to perform embossing, as shown in Figure 1. Subsequently, the glass covered by AAO template was heated to 80 °C for 10 min and then kept at 180 °C 60 min for solidification. After cooled to room temperature, the glass was successively placed in 5 wt% H₃PO₄ solution at 45 °C for 1 h to remove the back AAO layer, 23 wt% CuCl₂ + 8.5 wt% HNO₃ aqueous solution at room temperature for 5 min to remove the intermediate Al base, and again 45 °C, 5 wt% H₃PO₄ solution for 1 h to remove the effective AAO layer. Finally, SiO₂ nano-pillar array on glass surface was obtained.

Fluoroalkylsilane (FAS) modification was implemented by chemical vapor deposition according to reference [17], using 97% perfluorodecyltrichlorosilane as FAS reagent. Before FAS modification, UV-O₃ irradiation was conducted as pretreatment.

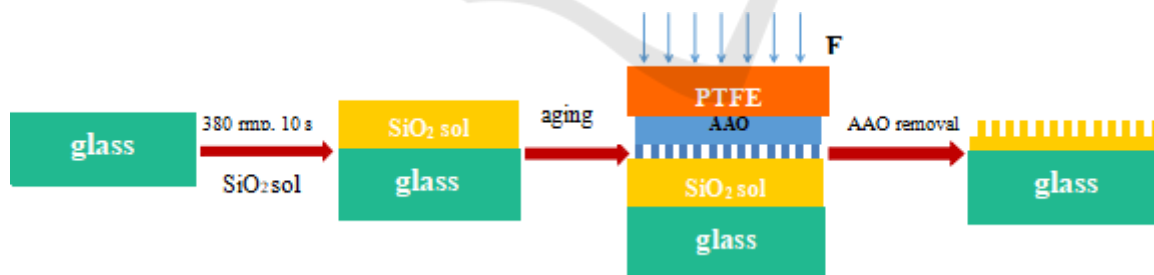


Figure 1. AAO imprinting process.

Contact angle meter (DGD-ADR, 8 μL water droplet, tangent method, room temperature) was used to measure static water contact angle (WCA) and roll angle (RA) of as-prepared SiO₂ nano-pillar structural surface. Scanning electron microscope (SEM, Hitachi SU-70, 5 kV) was used for morphology and structure characterization after gold coating (approximately 10 nm thickness). Visible light transmittance spectra were recorded by UV-Vis-NIR spectrometer (Lambda 750, Perkin Elmer) to characterize optical properties. In addition, atomic force microscope (AFM, nanoscope multimode VIII, DNP-10 tips, tapping mode) was used to measure surface roughness.

3. Results and discussion

Anodized nanoporous alumina oxide (AAO) with honeycomb structure consists of closely packed hexagonal cylinders of alumina cells, each with a circular pore in the middle. The model of “sp-100-40-150” AAO template represents that AAO layer contained regularly arranged nanopores with pore spacing of 100 nm, pore diameter of 40 nm, and pore depth of 150 nm. Figure 2. shows SEM micrographs of AAO template sp-100-40-150. From SEM top view (Figure 2a), the measured average pore spacing is 101.94 nm and average pore diameter is 43.01 nm, and from SEM cross-section view (Figure 2b), the pore depth is 150 nm, which is basically the same as the model.

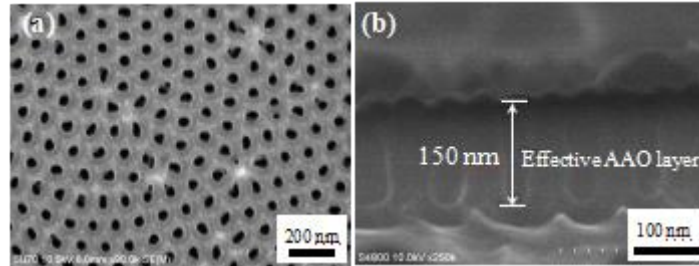


Figure 2. SEM micrographs of AAO template of sp100-40-150, (a) top view of effective AAO layer; (b) cross-section view of effective AAO layer.

According to Choi [18], longer nanopillars (aspect ratio >10) tend to clump together and form collapsed aggregation after AAO templates are chemically etched. In this work, AAO templates with a small pore depth (150 nm) were selected in order to prevent collapse of nanopillars and ensure visible light transmission of rough surface. Under the condition of same pore depth of 150 nm, AAO templates with different pore diameters were used, and a series of vertical nano-pillar arrays were obtained. SEM morphologies of SiO₂ nano-pillar arrays obtained by templates with the pore diameters of 40 nm (template “sp 100-40-150”), 60 nm (template “sp 125-60-150”), 80 nm (template “sp125-80-150”) and 100 nm (template “sp125-100-150”) are shown in Figure 3(a)(a’), (b)(b’), (c)(c’) and (d)(d’), respectively. The as-prepared SiO₂ nano-pillars are regular arrays, as shown in Figure 3., and average diameters of SiO₂ nanopillars are measured to be 48.78 nm, 72.73 nm, 87.98 nm and 104.90 nm, respectively, which correspond to pore sizes of the templates used.

Cassie and Baxter give a defined equation of apparent contact angle with a droplet on a composite surface [19], as shown below:

$$\cos \theta_w = f_1 \cos \theta_1 + f_2 \cos \theta_2 \quad (1)$$

Here, θ_w is apparent contact angle of a composite surface; f_1 and f_2 are area fractions of two media on the contact surface respectively, and $f_1 + f_2 = 1$; θ_1 and θ_2 are intrinsic contact angles on the two media respectively. When one of the media is air, the gas-liquid contact angle is 180° ($\theta_2 = 180^\circ$), and the above equation becomes:

$$\cos \theta_w = f_1(1 + \cos \theta_1) - 1 \quad (2)$$

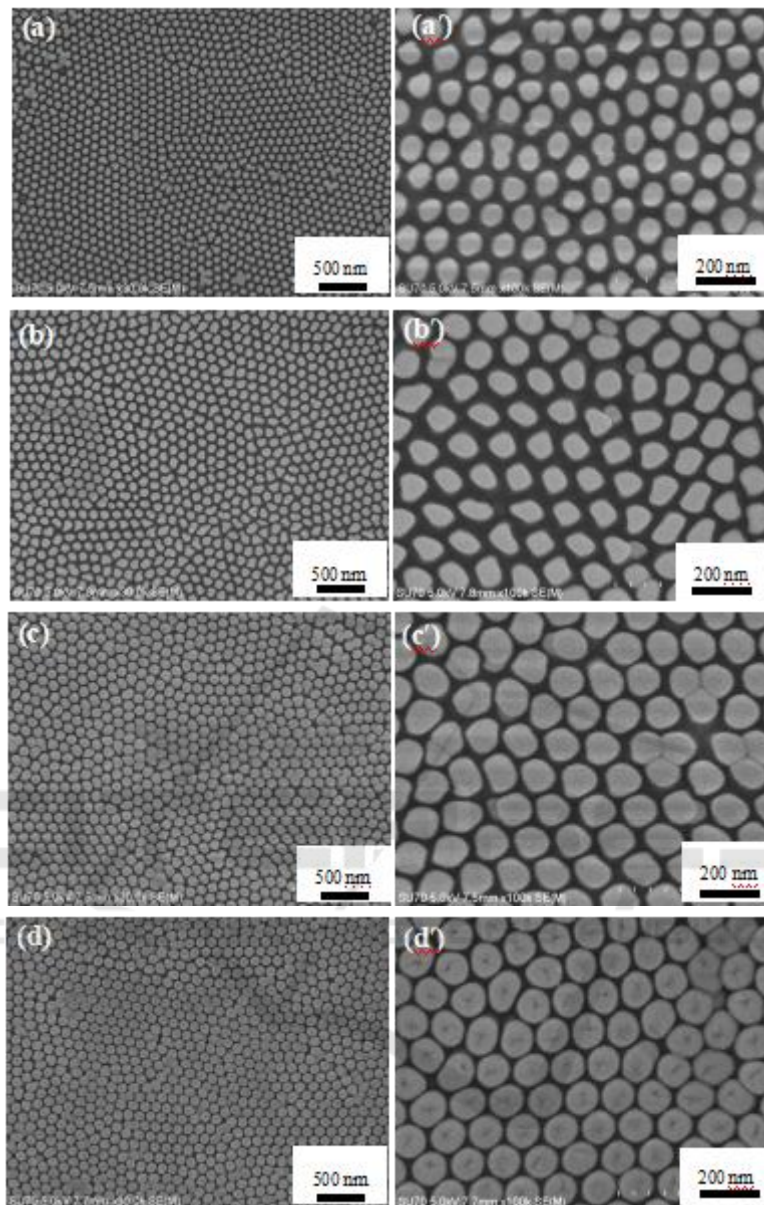


Figure 3. SEM micrographs of AAO – imprinted SiO₂ nanopillar arrays by different pore size templates: (a)(a') sp100-40-150, (b)(b') sp125-60-150, (c)(c') sp125-80-150, (d)(d') sp125-100-150. (a)(b)(c)(d): 30K magnification, (a')(b')(c')(d'): 100K magnification.

Wherein, f_1 is area fraction of solid surface in contact with water and always less than 1; θ_1 is intrinsic angle on the solid surface. According to equation (2), when $\theta_1 > 90^\circ$, the smaller the value of f_1 , the larger the apparent contact angle θ_0 is.

The theoretical apparent contact angle (θ_0), measured static water contact angle (measured WCA), measured rolling angle (measured RA) and water droplet state diagram are listed in Table 1. Here, the f_1 in Table 1. is calculated according to measured average diameters of SiO₂ nanopillars. In Table 1., sample "flat coating" is FAS-modified SiO₂ sol coating without AAO template embossing, which measured WCA (107°) can be used for the intrinsic contact angle θ_1 of SiO₂ nano-pillar arrays. Table 1. shows that: (1) the SiO₂ nano-pillar array by a template with the pore diameter of 43.01 nm has a

measured WCA of 150.47° and a measured RA < 5°, showing superhydrophobicity; (2) with the increase of average diameter of SiO₂ nanopillars, the static water contact angle gradually decreases, and the dynamic wetting property also gradually deteriorates; (3) measured WCA is basically consistent with theoretical θ_w , and hydrophobicity of SiO₂ nano-pillar arrays can be controlled by changing pore diameter of AAO templates.

Table 1. Comparisons between theoretical θ_w and measured WCA of SiO₂ nano-pillar array.

Samples	Pore spacing/nm	Pore diameter/nm	f_1	θ_w	Measured WCA	Measured RA	Water droplet state
Flat coating	\	\	\	\	107°	85°	
100-40-150	101.45	48.78	19.97%	149.17°	150.47°	<5°	
125-60-150	130.43	72.73	28.20%	143.17°	145.38°	20°	
125-80-150	131.97	87.98	41.26%	135.08°	137.11°	46°	
125-100-150	131.12	104.90	58.66%	125.80°	128.35°	55°	

AFM image of SiO₂ nano-pillar array of sample 100-40-150 is shown in Figure 4. Nanopillars are regular arrays, which is consistent with SEM result (Figure 3.). In 1 $\mu\text{m} \times 1 \mu\text{m}$ scan size, surface roughness (Ra) is 33.1 nm and maximum fluctuation (Rmax) is 179 nm. AFM results of surface roughness and maximum fluctuation are listed in Table 2. Figure 5. shows the relationship of Ra and Measured WCA, θ_w . With the increase of pore size of AAO templates, the roughness (Ra) of nano-pillar arrays decreases, which results in the decrease of measured WCA and θ_w .

Table 2. AFM test results of samples.

Samples	Ra\nm	Rmax\nm
100-40-150	33.1	179
125-60-150	17.2	164
125-80-150	13.5	146
125-100-150	7.0	56

The transmittance spectrum of sample 100-40-150 is shown in Figure 6., comparing with blank glass and glass with SiO₂ flat coating. The VIS transmittances (TL) of blank glass, glass with SiO₂ flat coating and glass with SiO₂ nano-pillar array (sample 100-40-150) are 74.91%, 75.50% and 78.55%, respectively. TL of sample 100-40-150 increases by 3.64% compared to the blank glass, because that the sub-wavelength-sized cylindrical structure with a feature size smaller than VIS wavelength can produce an effective refractive index gradient between air and nano-pillar array, resulting in reflection reduce and transmittance increase [12].

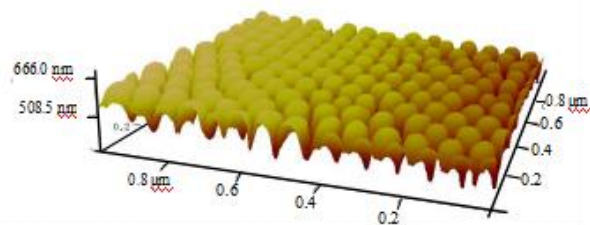


Figure 4. AFM image of the sample 100-40-150.

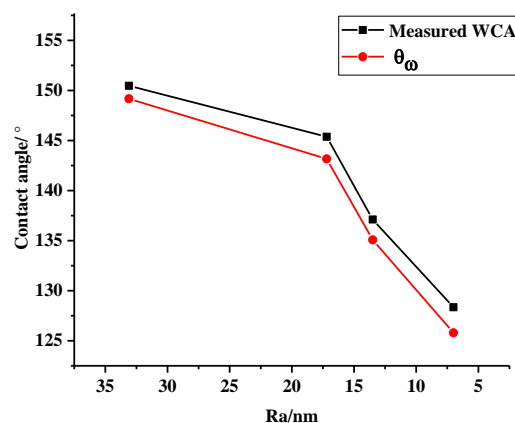


Figure 5. The relationship of Ra and Measured WCA, θ_w .

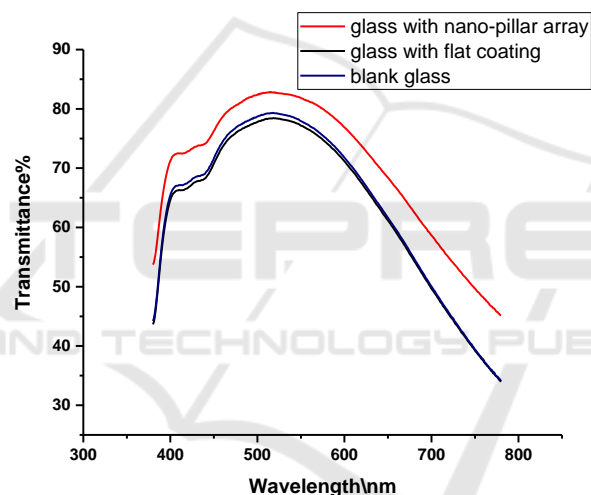


Figure 6. Transmittance spectra of blank glass, glass with SiO₂ flat coating and glass with SiO₂ nano-pillar array (sample 100-40-150).

4. Conclusions

In this work, inorganic SiO₂ nano-pillar arrays were prepared on glass surface by template imprinting method using AAO as template and SiO₂ sol as coating material. The diameter and surface roughness of SiO₂ nanopillars can be effectively controlled by changing pore size of template. This is a novel and facile method to prepare SiO₂ nano-pillar structural surface on glass substrate, presenting a new way to prepare super-hydrophobic self-cleaning glass.

Acknowledgement

This work is supported by the Science and Technology Major Program of Fujian Province (2014HZ0005), China.

References

- [1] Li X M, Reinhoudt D and Crego-Calama M 2007 *What do we need for a superhydrophobic*

- surface? A review on the recent progress in the preparation of superhydrophobic surfaces *J. Chemical Society Reviews* **36(8)** 1350-1368
- [2] Wang S, Liu K, Yao X and Jiang L 2015 *Bioinspired surfaces with superwettability: new insight on theory, design, and applications J. Chemical reviews* **115(16)** 8230-8293
- [3] Bayer I S 2017 On the durability and wear resistance of transparent superhydrophobic coatings *J. Coatings* **7(1)** 12
- [4] Zhang Y L, Xia H, Kim E and Sun H B 2012 *Recent developments in superhydrophobic surfaces with unique structural and functional properties J. Soft Matter* **8(44)** 11217-11231
- [5] Barthlott W and Neinhuis C 1997 *Purity of the sacred Lotus, or escape from contamination in biological surfaces J. Planta* **202(1)** 1-8
- [6] Huang W H and Lin C S 2014 *Robust superhydrophobic transparent coatings fabricated by a low-temperature sol-gel process J. Applied Surface Science* **305** 702-709
- [7] Chen Y, Zhang Y B, Shi L, Li J, Xin Y, Yang T T and Guo Z G 2012 *Transparent superhydrophobic/superhydrophilic coatings for self-cleaning and anti-fogging J. Applied Physics Letters* **101(3)** 033701
- [8] Xu Q F, Wang J N, Smith I H and Sanderson K D 2009 *Superhydrophobic and transparent coatings based on removable polymeric spheres J. Journal of Materials Chemistry* **19(5)** 655-660
- [9] Ganesh V A, Dinachali S S, Raut H K, Walsh T M, Nair A S and Ramakrishna S 2013 *Electrospun SiO₂ nanofibers as a template to fabricate a robust and transparent superamphiphobic coating J. RSC Advances* **3(12)** 3819-3824
- [10] Kim Y D, Shin J H, Cho J Y, Choi H J and Lee H 2014 *Nanosized patterned protective glass exhibiting high transmittance and self-cleaning effects for photovoltaic systems J. physica status solidi (a)* **211(8)** 1822-1827
- [11] Cho W K and Choi I S 2008 *Fabrication of hairy polymeric films inspired by geckos: wetting and high adhesion properties J. Advanced Functional Materials* **18(7)** 1089-1096
- [12] Liu Y, Song Y, Niu S, Zhang Y, Han Z and Ren L 2016 *Integrated super-hydrophobic and antireflective PDMS bio-templated from nano-conical structures of cicada wings J. RSC Advances* **6(110)** 108974-108980
- [13] Son J, Kundu S, Verma L K, Sakhuja M, Danner A J, Bhatia C S and Yang H 2012 *A practical superhydrophilic self cleaning and antireflective surface for outdoor photovoltaic applications J. Solar Energy Materials and Solar Cells* **98** 46-51
- [14] Liu K, Du J, Wu J and Jiang L 2012 *Superhydrophobic gecko feet with high adhesive forces towards water and their bio-inspired materials J. Nanoscale* **4(3)** 768-772
- [15] Lee W, Jin M K, Yoo W C and Lee J K 2004 *Nanostructuring of a polymeric substrate with well-defined nanometer-scale topography and tailored surface wettability J. Langmuir* **20(18)** 7665-7669
- [16] Shen K B, Yang H, Liu J, Wang W, Huang Y, Zhou Z H and Shen S 2012 *Fabrication and characterization for innate super-hydrophilic SiO₂ thin films J. Materials Science Forum* **743-744** 377-381
- [17] Liu X and He J 2009 *One-step hydrothermal creation of hierarchical microstructures toward superhydrophilic and superhydrophobic surfaces J. Langmuir* **25(19)** 11822-11826
- [18] Choi H, Lee S, Park S H, Ko J S and Yang H 2017 *Water repellency of large-scale imprinting-assisted polymer films J. Macromolecular Research* **25(6)** 584-590
- [19] Cassie A B D and Baxter S 1944 *Wettability of porous surfaces J. Transactions of the Faraday society* **40** 546-551